At5PTase13 Modulates Cotyledon Vein Development through Regulating Auxin Homeostasis[1][W]

Wen-Hui Lin, Yuan Wang, Bernd Mueller-Roeber, Charles A. Brearley, Zhi-Hong Xu, and Hong-Wei Xue*

National Key Laboratory of Plant Molecular Genetics, Institute of Plant Physiology and Ecology, Shanghai Institutes for Biological Sciences, Chinese Academy of Sciences, 200032 Shanghai, People's Republic of China (W.-H.L., Y.W., Z.-H.X., H.-W.X.); Partner Group of the Max-Planck-Institute of Molecular Plant Physiology on Plant Molecular Physiology and Signal Transduction, 200032 Shanghai, People's Republic of China (W.-H.L., Y.W., H.-W.X.); University of Potsdam, Institute of Biochemistry and Biology, D–14476 Golm, Germany (B.M.-R.); and School of Biological Sciences, University of East Anglia, Norwich NR4 7TJ, United Kingdom (C.A.B.)

Phosphatidylinositol signaling pathway and the relevant metabolites are known to be critical to the modulation of different aspects of plant growth, development, and stress responses. Inositol polyphosphate 5-phosphatase is a key enzyme involved in phosphatidylinositol metabolism and is encoded by an *At5PTase* gene family in *Arabidopsis thaliana*. A previous study shows that At5PTase11 mediates cotyledon vascular development probably through the regulation of intracellular calcium levels. In this study, we provide evidence that At5PTase13 modulates the development of cotyledon veins through its regulation of auxin homeostasis. A T-DNA insertional knockout mutant, *At5pt13-1*, showed a defect in development of the cotyledon vein, which was rescued completely by exogenous auxin and in part by brassinolide, a steroid hormone. Furthermore, the mutant had reduced auxin content and altered auxin accumulation in seedlings revealed by the DR5:β-glucuronidase fusion construct in seedlings. In addition, microarray analysis shows that the transcription of key genes responsible for auxin biosynthesis and transport was altered in *At5pt13-1*. The *At5pt13-1* mutant was also less sensitive to auxin inhibition of root elongation. These results suggest that At5PTase13 regulates the homeostasis of auxin, a key hormone controlling vascular development in plants.

The plant vascular network is complex and critical for plant growth and development, but the mechanisms underlying vascular development and vein patterning in leaves and cotyledons are poorly understood. Due to its relatively simple structure, the cotyledon vein provides an ideal model for studying vascular development and vein patterning. Arabidopsis (*Arabidopsis thaliana*) cotyledon veins consist of the midvein (from the petioles to the cotyledons), the distal secondary veins (two distal arcs), the proximal secondary veins (two proximal arcs near the petiole), and the distal and proximal areoles (normally four areoles; Sieburth, 1999). The development of cotyledon veins consists of several steps: differentiation of the provascular tissues, transformation from provascular to procambium tissues, appearance of the secondary cell wall, and the venation formation (Ye and Varner, 1991).

Analyses of mutants with abnormal leaf or cotyledon veins, including *cvp* (cotyledon vascular pattern; Carland et al., 1999, 2002), *sfc* (scarface; Deyholos et al., 2000), *axr6* (auxin-resistant 6; Hobbie et al., 2000), and *van* (vascular network; Koizumi et al., 2000) have expanded the knowledge of vein development and patterning. Mutations in *CVP1* cause misshapen vascular cells, while *cvp2* develops an unconnected vein and a discontinuous uniform pipeline, though the individual vascular cells appear normal. All known *cvp2* mutant alleles exhibit a discontinuous cotyledon venation pattern consisting of isolated patches of vascular tissues, additional extra loops, thicker cotyledon veins, and cotyledon expansion in the proximal-distal axis, resulting in a soup spoon-shaped cotyledon (Carland et al., 1999, 2002). *CVP2* is expressed in the procambium of cotyledons at the very early stages of embryonic development, leaves, and stems, suggesting *CVP2* is involved in the development of different types of vascular tissues (Carland and Nelson, 2004). In contrast, *SFC* is more specifically required for continuous patterning of secondary veins. Mutations in *SFC* induce abnormal vascular islands in cotyledons, in which the secondary veins were mostly replaced with short vein-like segments or vascular islands (Deyholos et al., 2000), indicating that SFC is

[1] This work was supported by the Chinese Academy of Sciences and National Natural Science Foundation of China (grant nos. 30425029 and 30421001).

* Corresponding author; e-mail hwxue@sibs.ac.cn; fax 86–21–54924060.

The author responsible for distribution of materials integral to the findings presented in this article in accordance with the policy described in the Instructions for Authors (www.plantphysiol.org) is: Hong-Wei Xue (hwxue@sibs.ac.cn).

[W] The online version of this article contains Web-only data.

Article, publication date, and citation information can be found at www.plantphysiol.org/cgi/doi/10.1104/pp.105.067140.

required for the formation of continuous cotyledon secondary vein patterning.

Evidence suggests that auxin plays a critical role in the formation of cotyledon veins. The *sfc* mutants exhibit increased sensitivities to exogenous auxin (Deyholos et al., 2000), and auxin-resistant mutants, e.g. *axr5* and *axr6*, show an incomplete vein pattern and defective development of vascular tissues (Hobbie et al., 2000). Studies employing polar auxin transport inhibitors indicate that the presence and polar transport of auxin are critical for vascular tissue development in cotyledons and leaves, especially the secondary and tertiary veins (Mattsson et al., 1999; Sieburth, 1999; Friml, 2003). Two different hypotheses have been proposed to explain how auxin is involved in vascular tissue development: (1) the auxin signal flow canalization hypothesis, based on experimental observation of the inductive effect of auxin on vascular tissue formation, and (2) the diffusion-reaction prepattern hypothesis, which is derived from computer modeling of interactions among hypothetical diffusible substances and positive feedback loops (Koizumi et al., 2000). However, the mechanism by which auxin modulates vascular development remains unclear. Furthermore, the mechanisms controlling auxin transport and accumulation during the cotyledon vein development are mysterious. Other phytohormones such as brassinosteroids (BRs) are also important for vascular development (Carland et al., 1999, 2002), but their mode of action and functional relationship to auxin are poorly understood.

The phosphatidylinositol (PI) signaling pathway participates in many developmental processes and cellular responses to environmental stimuli (Lin et al., 2004). Signaling molecules include phospholipids (PI phosphates) and soluble inositol phosphates. Inositol 1,4,5-trisphosphate [Ins(1,4,5)P_3] (produced by phosphoinositide-specific phospholipase C-mediated hydrolysis of PI 4,5-bisphosphate) and inositol 1,3,4,5-tetrakisphosphate [Ins(1,3,4,5)P_4] play central roles in signal transduction. Both Ins(1,4,5)P_3 and Ins(1,3,4,5)P_4 regulate the release of internal Ca^{2+} stores and uptake of extracellular Ca^{2+} in animal cells (Zhu et al., 2000; Pouillon et al., 2003). Ins(1,3,4,5)P_4 was excluded from the degradation products generated by endogenous phytase activity during phytate degradation assays (Hatzack et al., 2001). However, few reports have investigated the functions of Ins(1,3,4,5)P_4 in higher plants.

Ins(1,3,4,5)P_4 can be dephosphorylated by inositol polyphosphate 1-phosphatase (IPP1ase; Xiong et al., 2001) or 5-phosphatase (5PTase; Berdy et al., 2001; Sanchez and Chua, 2001; Burnette et al., 2003; Zhong and Ye, 2004), both of which have been identified in plant cells. Phenotypic analyses of the relevant mutants indicated the involvement of IPP1ase in salt tolerance (Xiong et al., 2001), and the importance of 5PTase in abscisic acid (ABA) responses (Sanchez and Chua, 2001; Burnette et al., 2003) and cotyledon vein development (Carland and Nelson, 2004). Biochemical analyses showed that Arabidopsis 5PTases have phosphatase activity against different substrates including Ins(1,4,5)P_3 and Ins(1,3,4,5)P_4, phosphatidylinositol 4,5-bisphosphate, phosphatidylinositol 3,5-bisphosphate, and phosphatidylinositol 3,4,5-trisphosphate (Berdy et al., 2001; Ercetin and Gillaspy, 2004; Zhong et al., 2004; Zhong and Ye, 2004), similar to those in animal cells (Erneux et al., 1998). Different 5PTases have different substrate specificity, suggesting the presence of different types of 5PTases with distinct biological functions. Recent analysis revealed that *cvp2* (with open vein networks and free vein endings) was due to a deficiency in At5PTase11 (Carland et al., 1999; Carland and Nelson, 2004), indicating that At5PTase11 and the PI signaling pathway are involved in vascular tissue development. Ins(3,4,5)P_3 levels are elevated in the *cpv2* mutant, suggesting a potential involvement of Ins(3,4,5)P_3-mediated cytosolic calcium in the regulation of vascular development.

In this study, we demonstrate that an At5PTase knockout mutant exhibits a defect in cotyledon vein development and patterning, but this defect is distinct from that induced by *cvp2* (*At5PTase11*) mutations. Furthermore, we show that this defect is rescued by exogenous auxin and that the At5PTase13 mutant has reduced auxin levels and altered expression of auxin-regulated genes. These results suggest that At5PTase has a function distinct from that of At5PTase11 and modulates vascular development through the regulation of auxin homeostasis.

RESULTS

Isolation of At5PTase13, an Arabidopsis Inositol Polyphosphate 5PTase Containing Multiple WD40 Repeats

An Arabidopsis cDNA (accession no. AC007153) was identified by homologously searching the National Center for Biotechnology Information database with a cDNA encoding a putative inositol polyphosphate phosphatase (AJ005682). Specific primers located in the predicted first exon were designed and used to screen an Arabidopsis hypocotyl cDNA library. We obtained an apparent full-length cDNA of 4,032 bp encoding a 1,094 amino acid polypeptide with a molecular mass of approximately 120 kD, named At5PTase13. Comparison of the cDNA with genomic sequences revealed the presence of 10 exons (80–800 bp) and nine introns (80–330 bp; Fig. 1A). The annotated gene structure in the database was essentially correct except for alterations in the sixth (one additional 104-bp intron was predicted) and final exons (the predicted exon is 227 bp longer). *At5PTase13* is located on chromosome 1 (locus no. At1g05630) and presented in a single copy in the genome. During the manuscript preparation, Zhong et al. (2004) reported the molecular and biochemical characterization of At5PTase13, confirming its inositol polyphosphate phosphatase activity specifically toward Ins(1,4,5)P_3.

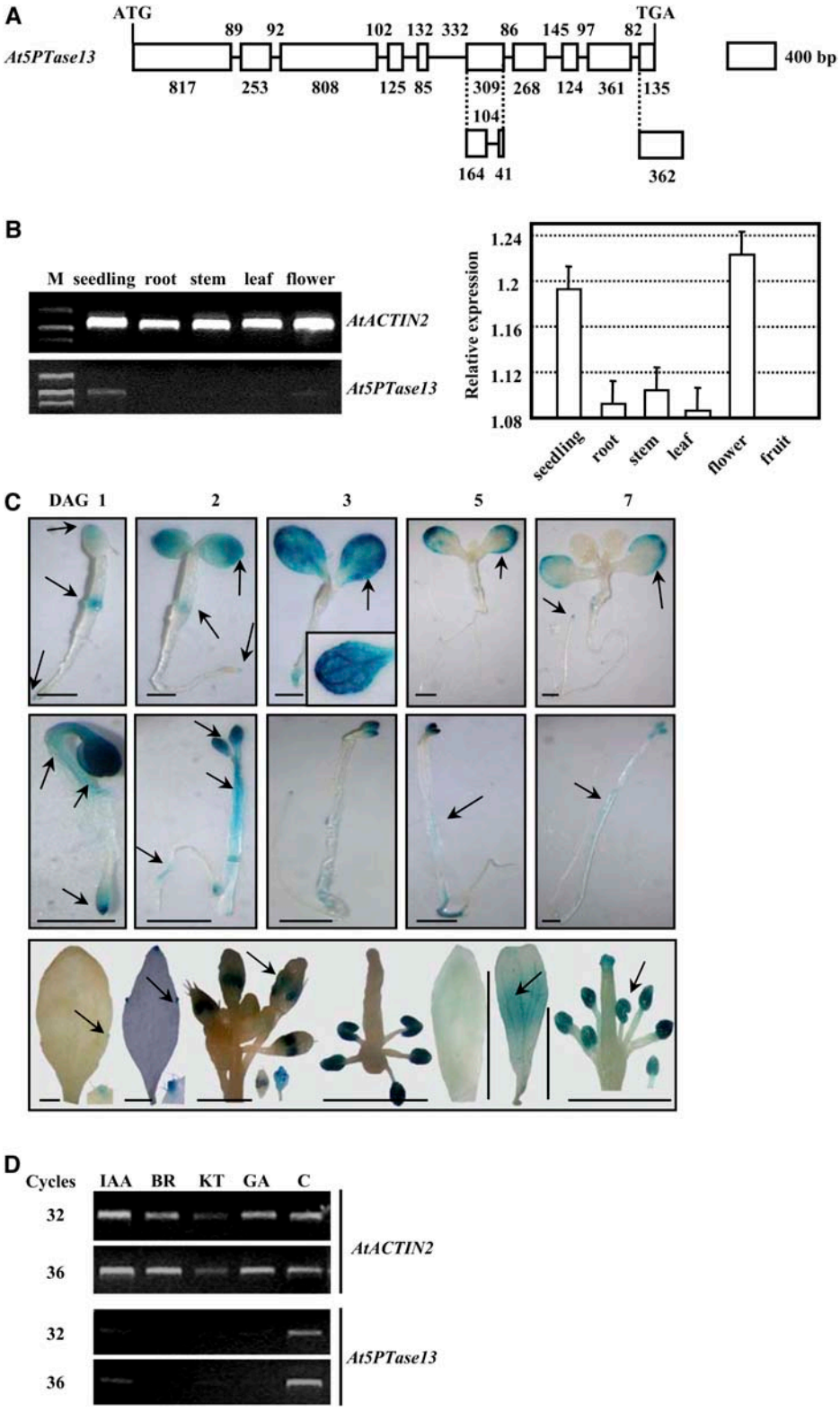

Figure 1. Structure and expression of *At5PTase13*. A, Gene organization of *At5PTase13*. Numbers represent the sizes of the exons and introns. The computational predictions for the sixth (one 104-bp intron was predicted) and last (the prediction is 227 bp longer) exons were incorrect (bottom section). B, Semiquantitative RT-PCR analysis shows that *At5PTase13* is mainly expressed in young seedlings, with weak transcripts in flowers and almost no expression in roots, stems, and leaves (left section). Further analysis via quantitative real-time RT-PCR confirmed the relatively higher expression of *At5PTase13* in young seedlings and flowers, while lower expression in fruit, roots, stems, and leaves (right section). Data presented are compared with *AtACTIN2* and shown as percentage. Bars indicate SD. C, Promoter-reporter (GUS) fusion studies demonstrate the *At5PTase13* expression in the tips of cotyledons, root tip, and hypocotyls-root juncture at day 1 after germination, and then expand to the whole cotyledon. At days 3 and 5, the expression was concentrated at the pinnacle of cotyledons. Later (days 5–7, when the first two pairs of true leaves appeared), the expression of *At5PTase13* decreased and was focused in cotyledon margin and root tip. *At5PTase13* exhibited stronger expression in seedlings grown in darkness (middle section) and is also detected in inflorescence leaves, petals, and pollen grains, but weakly in sepal and rosette leaves (bottom section). Arrows show the positions of *At5PTase13* expression. A few expression patterns are highlighted in rectangles. Bar = 1 mm. D, Semiquantitative RT-PCR analysis revealed that *At5PTase13* was down-regulated following treatment with different plant hormones. Seven-day-old seedlings were treated with 100 μM auxin (IAA), cytokinin (Kinetin), GA (GA_3), or 1 μM 24-eBL for 8 h.

At5PTase13 Is Expressed in Young Seedlings and Regulated by Phytohormones

Semiquantitative reverse transcription (RT)-PCR analysis revealed that *At5PTase13* was expressed in young seedlings and flowers, while no transcripts were detectable in maturated roots, stems, and rosette leaves (Fig. 1B, left section). Further analysis via real-time quantitative PCR confirmed the relatively higher expression of *At5PTase13* in seedlings and flowers,

while lower expression in fruits (Fig. 1B, right section). To further characterize *At5PTase13* expression pattern, we fused the 1.4-kb *At5PTase13* promoter region to the *Escherichia coli* β-glucuronidase (GUS) coding gene and transformed the resulting construct (pBI101-P) into Arabidopsis plants. T-DNA integration into the plant genome was confirmed by PCR analysis and five independent positive lines were identified (data not shown). In young seedlings, *At5PTase13*:*GUS* expression was detected in cotyledons prior to seed germination, and was expanded to root tips and juncture of hypocotyl. The maximal GUS expression of *At5PTase13* was restricted to the cotyledon tips until 2 d after seed germination. On days 3 and 4, GUS was detected in the cotyledons or cotyledon veins. A similar pattern was detected on days 5 and 7, though the expression level was decreased. In addition, *At5PTase13*:*GUS* expression was observed at the cotyledons margin, juncture of hypocotyl and root, and root tips (Fig. 1C, top section). When the first pair of vegetative true leaves appeared around day 5, *At5PTase13*:*GUS* expression in cotyledons was reduced. Interestingly, the expression pattern of *At5PTase13*:*GUS* was very similar to auxin distribution in seedlings as indicated by a *DR5*:*GUS* expression (Fig. 3A).

At5PTase13:*GUS* activities were also detected in the apex of inflorescence (Fig. 1C, bottom section). *At5PTase13*:*GUS* was expressed in the hydratodes of inflorescence curling leaves, weakly expressed in sepal (relatively high in petal), and highly expressed in anther and pollen grains, but was not expressed in pistils.

Computational analysis of the *At5PTase13* promoter region (http://www.dna.affrc.go.jp/htdocs/PLACE/signalscan.html) revealed the presence of potential cis-elements for auxin and blue light/UV responses, which is consistent with the observation that *At5PTase13* expression was suppressed by auxin (Fig. 1D) and stimulated by darkness (Fig. 1C, middle section), especially in the hypocotyls on days 1 to 2 after germination. In addition, treatments of seedlings with plant hormones such as cytokinin, GA, and brassinolide (BL) suppressed *At5PTase13* expression (Fig. 1D).

At5PTase13 Deficiency Results in Abnormal Cotyledon Vein Development

To study the physiological role of At5PTase13, a putative T-DNA insertion line, Garlic 350-F1, termed as *At5pt13-1*, was identified using the *At5PTase13* genomic sequence to search against the flanking sequence database of Arabidopsis mutant populations by Syngenta (Torrey Mesa Research Institute, Syngenta Research and Technology; the Syngenta Arabidopsis Insertion Library or SAIL, formerly known as GARLIC). The putative insertion site was in the fourth exon of the At5PTase13 gene (Fig. 2A), which was confirmed by PCR amplification using primers located in the T-DNA (LB3) and flanking genomic regions (Fig. 2B, left). Segregation ratio analysis of herbicide resistance (with a ratio of 3.04:1 of resistant:sensitive, in total 93 seedlings) and phenotypic observations (with a ratio of 1:1.94 of abnormal:normal seedlings, in total 53 seedlings) indicates the presence of a single T-DNA insertion, and that *At5pt13-1* is a recessive mutation. Both heterozygous and homozygous plants were confirmed by PCR amplification using primers located in the T-DNA and flanking genomic regions (Fig. 2B, right). As expected, *At5PTase13* transcript was not detected in the homozygous *At5pt13-1* mutants (Fig. 2C).

According to the expression pattern of *At5PTase13*, we focused our observations on cotyledon development, especially the vascular tissues. There is no obvious growth difference between *At5pt13-1* and wild-type seedlings, while the development of vascular tissues was obviously altered in *At5pt13-1* (Table I). In wild-type plants, the primary vascular tissues of the cotyledons are clearly observed on day 2 after germination, and the secondary ones form 2 or 3 d later, with approximately symmetrical, continuous architectures and slick veins (Sieburth, 1999; Deyholos et al., 2000). Some proximal secondary veins do not close to the intending point in wild-type seedlings. A very low percentage (less than 1%) of the cotyledon veins is incomplete, anisomerous, or in incorrect orientation to the intending point in wild-type plants. Compared to wild-type plants (Fig. 2D, b), cotyledon veins of *At5pt13-1* were with altered numbers (4%; Fig. 2D, b and c), in incorrect vein orientation (16.3%; Fig. 2D, d and e), with additional or altered loops (1.7%; Fig. 2D, f–h), with branches (1.3%; Fig. 2D, i and j), with intersections (1.3%; Fig. 2D, k) and fusions (5.3%; Fig. 2D, l) of the distal and proximal secondary veins, or with acute angles (3.3%; Fig. 2D, m). In addition, the cotyledon veins of *At5pt13-1* were asymmetric, with flexed secondary veins and often multiple abnormalities, such as asymmetry, abnormal caecal orientation, or flex (10.7%). Statistical analyses revealed that around 64.7% of the total cotyledons showed obvious abnormality, while the ratio of seedlings with abnormal cotyledons reaches to approximately 90% (Table I).

To investigate whether At5PTase is involved in the patterning of cotyledon veins or the differentiation of vascular cells, we examined the architecture and formation of cotyledon veins using differential interference contrast optics and cross sections. We found that the veins in the mutants, especially the secondary veins, were coarser than those in wild-type seedlings (Fig. 2D, o and q). However, the vascular cells did not show obvious cellular changes, suggesting At5PTase primarily modulates cotyledon vein patterning.

At5PTase13 Could Complement the Abnormal Cotyledon Vein Development of *At5pt13-1*

To test whether the abnormal cotyledon vein patterns in *At5pt13-1* are indeed due to the disruption of the *At5PTase13* gene, a construct harboring *At5PTase13* under its native promoter (pBI101-P-At5PTase13) was

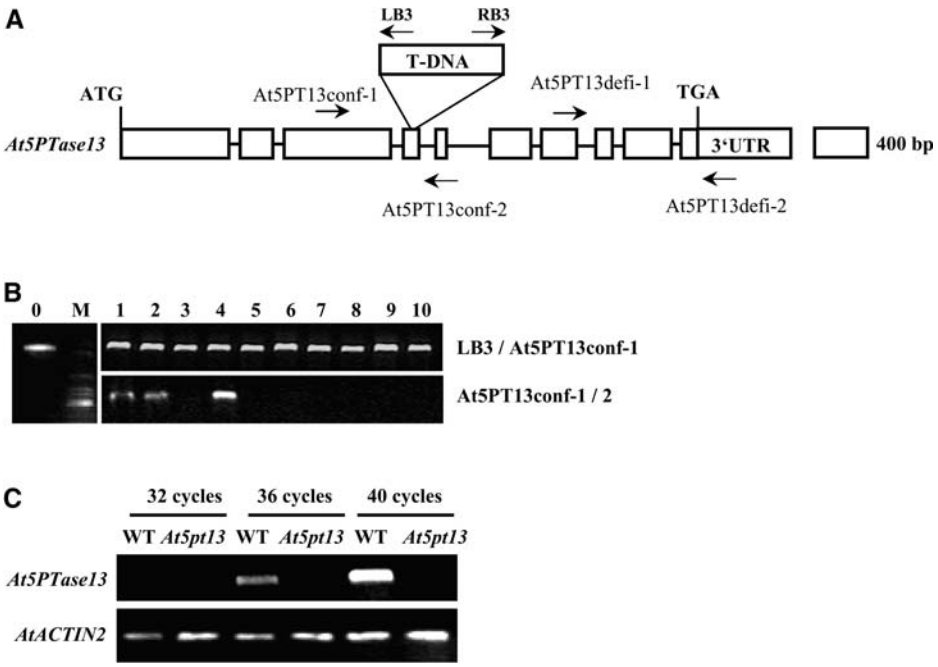

Figure 2. Identification and analysis of *At5PTase13* deficiency mutants. A, A single T-DNA insertion in the fourth exon of *At5PTase13* in the *At5pt13-1* mutant. The positions of primers used to confirm T-DNA (At5PT13conf-1 and 2) in the *At5PTase13* gene and deficiency of *At5PTase13* (At5PT13defi-1 and 2) are indicated. B, Confirmation of T-DNA insertion (left section) and identification of homozygous lines (right section). T-DNA insertion was confirmed (lane 0) by PCR amplification using primers At5PT13conf-1 (located in the 5′ flanking region) and LB3. Homozygous lines were further identified via PCR amplification through primers At5PT13conf-1 and 2, which are located in the 5′ and 3′ flanked regions and show a positive signal only in the case of heterozygous lines (lanes 1, 2, and 4). C, Semiquantitative RT-PCR analysis with primers At5PT13defi-1 and 2 confirmed the absence of *At5PTase13* expression in *At5pt13-1*. RNA was extracted from 4-d-old seedlings, and PCR amplifications were performed for 32, 36, and 40 cycles. Arabidopsis actin coding gene was employed as a positive internal control. D, Growth of *At5pt13-1* seedlings. Compared to the cotyledon veins of wild-type seedlings (a, 4-d, mid-vein, and distal secondary vein developed), those of *At5pt13-1* showed various abnormal patterns (b–q), including altered numbers of veins (b and c), improper orientation (d and e), additional loops (f–h), branches (i and j), intersections of the distal and proximal secondary veins (k), fusion of the distal and proximal secondary veins at one side (l), acute angles (m), and coarse (o and q, comparing to that of wild-type plants, n and p). The abnormalities are highlighted by arrows. Vascular tissues were observed using differential interference contrast microscopy. Expression of *At5PTase13* in *At5pt13-1* rescued the abnormal cotyledon vein development (r), as did the application of exogenous NAA (0.1 μM; s, 2-d-old, and t, 4-d-old seedlings). E, Expression of *At5PTase13* was detected after transformation with the construct harboring *At5PTase13* under its own promoter (pBI101-P-At5PTase13). RNAs were extracted from 4-d-old seedlings and PCR amplification was performed for 36 cycles.

transformed into wild-type and homozygous *At5pt13-1*. Four independent transgenic lines with single T-DNA insertion were identified. Semiquantitative RT-PCR analysis confirmed the rescued expression of *At5PTase13* in these transformed *At5pt13* lines (Fig. 2E), and further microscopic analysis indicated that the cotyledon veins of transgenic seedlings were normal in the T1 and T2 generation plants (Fig. 2D, r). Statistical analysis showed that the frequencies of abnormal cotyledon veins were significantly reduced in the transformed plants (Table I), indicating that abnormal cotyledon vein development of *At5pt13-1* is due to the *At5PTase13* deficiency.

Exogenous Auxin and BL Rescue the Abnormal Cotyledon Vein Development in *At5pt13-1*

Both auxin and BRs are known to regulate the development of both leaf and cotyledon veins (Semiarti et al., 2001). We thus tested whether the abnormal cotyledon veins of *At5pt13-1* could be rescued by exogenous auxin or BR. Interestingly, the abnormal cotyledon veins were almost completely rescued by low concentrations of naphthylacetic acid (NAA; 0.1 μM; Fig. 2D, s and t) or in part by 24-epi-BL (24-eBL; 0.1 μM). Statistical analyses indicated that the frequency of NAA-treated or 24-eBL-treated *At5pt13-1* with abnormal cotyledon veins was reduced, i.e. from 90% to 15% and 39%, respectively (Table I). These results suggest that At5PTase13 is involved in the accumulation and distribution required for normal vascular patterning.

We next examined whether the *At5pt13-1* mutation alters the distribution and the level of auxin. Arabidopsis plants harboring *DR5*:*GUS* construct (Ulmasov et al., 1997) were employed, and a homozygous line of *DR5*:*GUS* and *At5pt13-1* was obtained by crossing. As shown in Figure 3A, *At5pt13-1* dramatically altered both the distribution and the level of *DR5*:*GUS*

Figure 2. (*Continued.*)

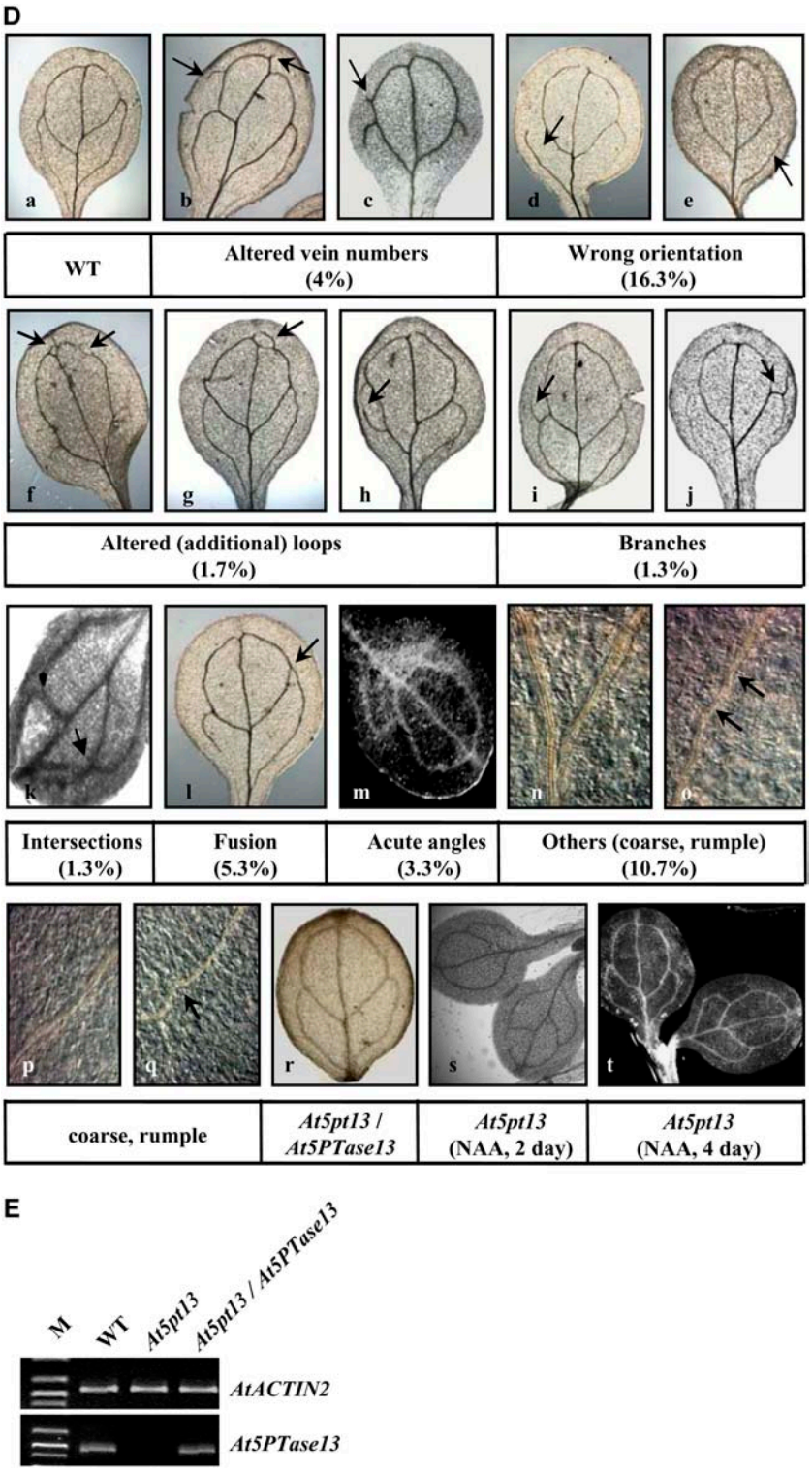

expression. GUS levels were reduced throughout the whole seedlings, especially in cotyledons at 1 to 2 d after germination, and the distribution was modified in root tissues (absent in the root tip but dispersed in the elongation zone). In 4-d-old seedlings, the GUS level in crossed offspring is much reduced compared to that in the controls. When exogenous auxin (NAA, 0.1 μM) was applied to *DR5:GUS/At5pt13-1* seedlings, GUS levels and distribution was recovered nearly to those in wild-type background, although the GUS levels were still relatively lower compared to wild type, especially at 4 d after germination (Fig. 3A).

Table I. *Statistical analysis of the cotyledon development of At5pt13-1*
Numbers indicate plants with abnormal cotyledons or the ratio of abnormal cotyledons.

Plants	Seedlings				
	Total	Two Normal Cotyledons	One Normal Cotyledon	Two Abnormal Cotyledons	Abnormality
Wild type	150	146	3	1	2.67%
0.01 μM IP_4 treatment	100	26	36	28	64%
At5pt13-1	150	15	76	59	90%
At5pt13-1 (0.1 μM NAA)	100	81	9	6	15%
At5pt13-1 (0.1 μM BR)	100	61	17	22	39%
At5pt13-1/pBI101-P-*At5PTase13*	100	78	7	15	22%

To assess whether the *At5pt13-1* indeed affected free auxin levels, we assayed free auxin using an ELISA method as described (Liang and Yin, 1994). As shown in Figure 3B, the auxin content in 4-d-old *At5pt13-1* seedlings is approximately half of that in wild-type ones, confirming that At5PTase13 modulates auxin accumulation.

Auxin Biosynthesis and Transport-Related Genes Are Modified in *At5pt13*

To explore the possible mechanism for At5PAse13 regulation of auxin accumulation and distribution, we examined whether *At5PTase13* affected the expression of auxin biosynthesis- and transport-related genes. Semiquantitative RT-PCR analysis shows that out of five auxin biosynthesis-related genes covering three different biosynthesis pathways (Bartel et al., 2001) and six transport-related genes (PIN1–4, 6, and 7; Friml, 2003), two showed modified transcript levels in *At5pt13-1* (Fig. 4A, top section). Real-time quantitative PCR analysis confirmed the unaltered expression of *NIT1* (Nitrilase 1; while *NIT*3 was enhanced; Table II) and stimulated expression of *CYP83B1* and *PIN4* (Fig. 4A, bottom section). Transcript level of *CYP83B1*, acting as an important branch point for auxin and glucosinolate biosynthesis, was increased in *At5pt13-1* (4-d-old seedlings). A loss-of-function mutant of *CYP83B1* (*sur2*) was previously reported to have a higher level of free auxin and a reduced glucosinolate level, while a transgenic line overexpressing *CYP83B1* had low auxin and high glucosinolate levels (Bak et al., 2001; Bartel et al., 2001). This is consistent with our observation that the amount of auxin is reduced in *At5pt13-1*. The increased expression of *PIN4*, which is responsible for maintaining the auxin gradient in roots and helps to initiate or stabilize an auxin feedback loop (Friml, 2003), suggests that auxin transport is also modified in *At5pt13-1* mutant plants, consistent with their altered auxin distribution.

To further investigate the possible mechanism of At5PTase13 action and to confirm the altered expression of auxin-related genes in the *At5pt13-1* mutant, we performed a global gene expression profiling of the 4-d-old aerial organs of wild-type and *At5pt13-1* seedlings using the whole-genome microarray chip (Affymetrix, ATH1). The hybridization results revealed altered expression of auxin biosynthesis- and signaling-related genes (Tables II and III). Under the *At5PTase13* deficiency, the expression of genes encoding proteins involved in auxin biosynthesis, especially those related to the Trp-dependant pathway and the indole glucosinolate branch (Bartel et al., 2001), was differentially modified. Among them, expression of *AAO1* (indole-3-acetaldehyde oxidase) and *CYP83B1* (cytochrome P450) was enhanced, while the expression of *NIT3*, *TRP2* (Trp synthase β), and *TRP3* (Trp synthase α) was suppressed (see Fig. 4B). In addition, about 30 auxin-related genes, coding for auxin-induced proteins or auxin-responsive factors, were affected (Table III). It was interesting to note that the BR biosynthesis-related genes were not modified in the *At5pt13-1* mutant except for *DWF4*, whose expression was slightly suppressed. Genes involved in cytokinin and GA metabolism were also affected, consistent with the RT-PCR analysis showing that cytokinin and GA suppress *At5PTase13* transcription. In addition to the hormone-related genes, genes encoding proteins participating in signal transduction (10% of the total regulated genes), transcription (8%), disease resistance (2%), metabolism (17%), photomorphogenesis (1%), and development (1%) exhibited altered expression in *At5pt13-1* (Supplemental Table I). Taken together, these results suggest the involvement of *At5PTase13* in multiple growth and developmental processes and responses to the environment.

At5pt13-1 Is Less Sensitive to Auxin and ABA

We also tested whether *At5pt13-1* altered auxin sensitivity. Root lengths of *At5pt13-1* seedlings on the medium supplemented with different concentrations of auxin (indole-3-acetic acid [IAA], 0.01, 0.1, 1, and 10 μM) were measured and the relative promotion and inhibition were calculated. The results show that, compared to the wild-type seedlings, *At5pt13-1* is less sensitive to exogenous IAA, especially at concentrations of 0.01, 0.1, and 1 μM (Fig. 5A). Microarray analysis described above indeed showed that auxin-related genes, including genes coding for auxin-regulated proteins and auxin-responsive factor-like

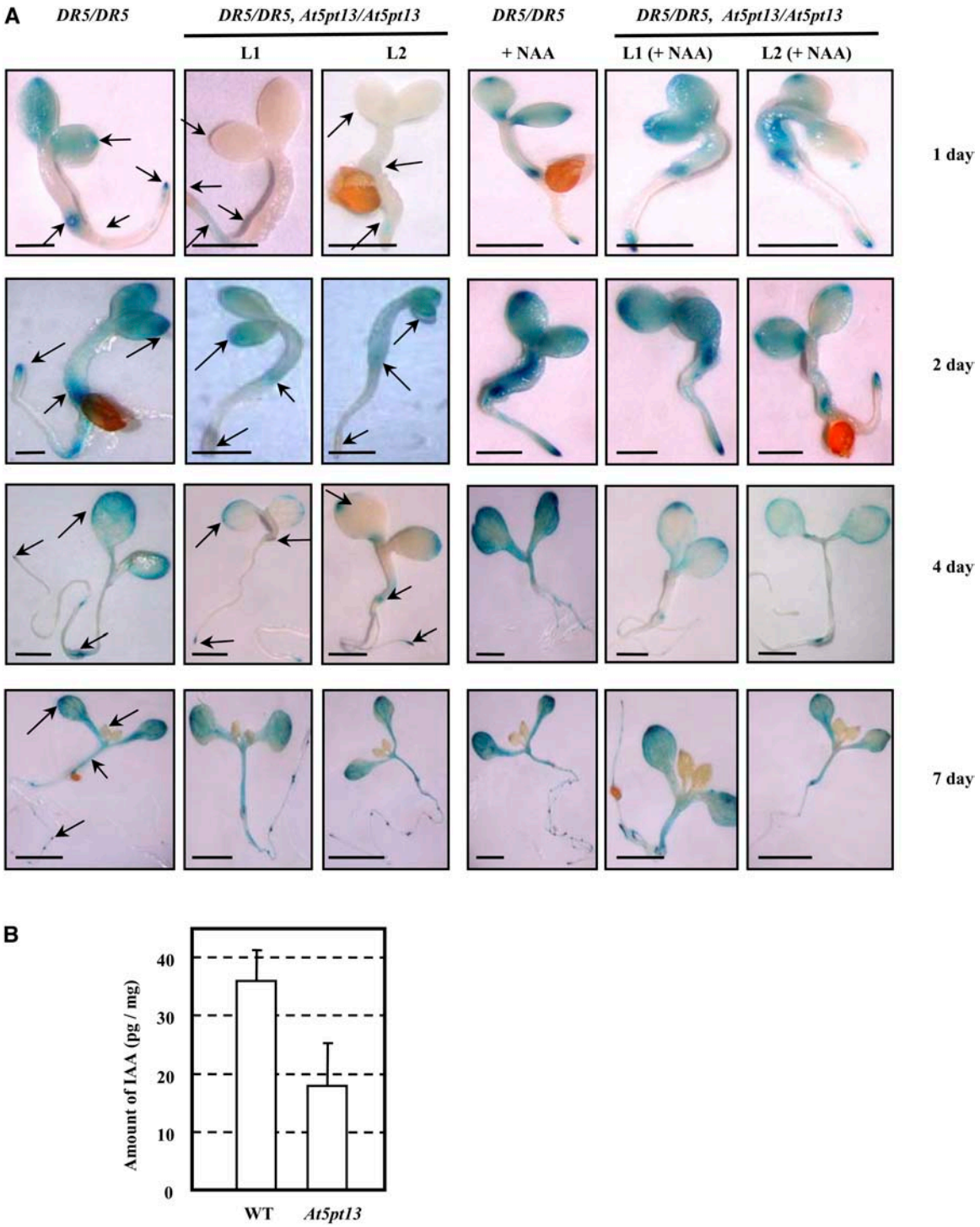

Figure 3. Altered auxin accumulation and distribution in *At5PTase13*-deficient plants. A, GUS activity detection of homozygous DR5:GUS/*At5pt13-1* cross offsprings implies altered auxin levels and distribution in *At5pt13-1* seedlings grown at 1, 2, and 4 d (two independent homozygous lines, L1 and 2) after germination. Adscititious NAA in low concentrations could enhance auxin levels in both DR5:GUS/*At5pt13-1* and control plants. Bar = 4 mm. B, Quantitative assay of free auxin content in wild-type and *At5pt13-1* seedlings. Four-day-old seedlings were used for ELISA analysis. The measurements were repeated four times and bars indicate SD.

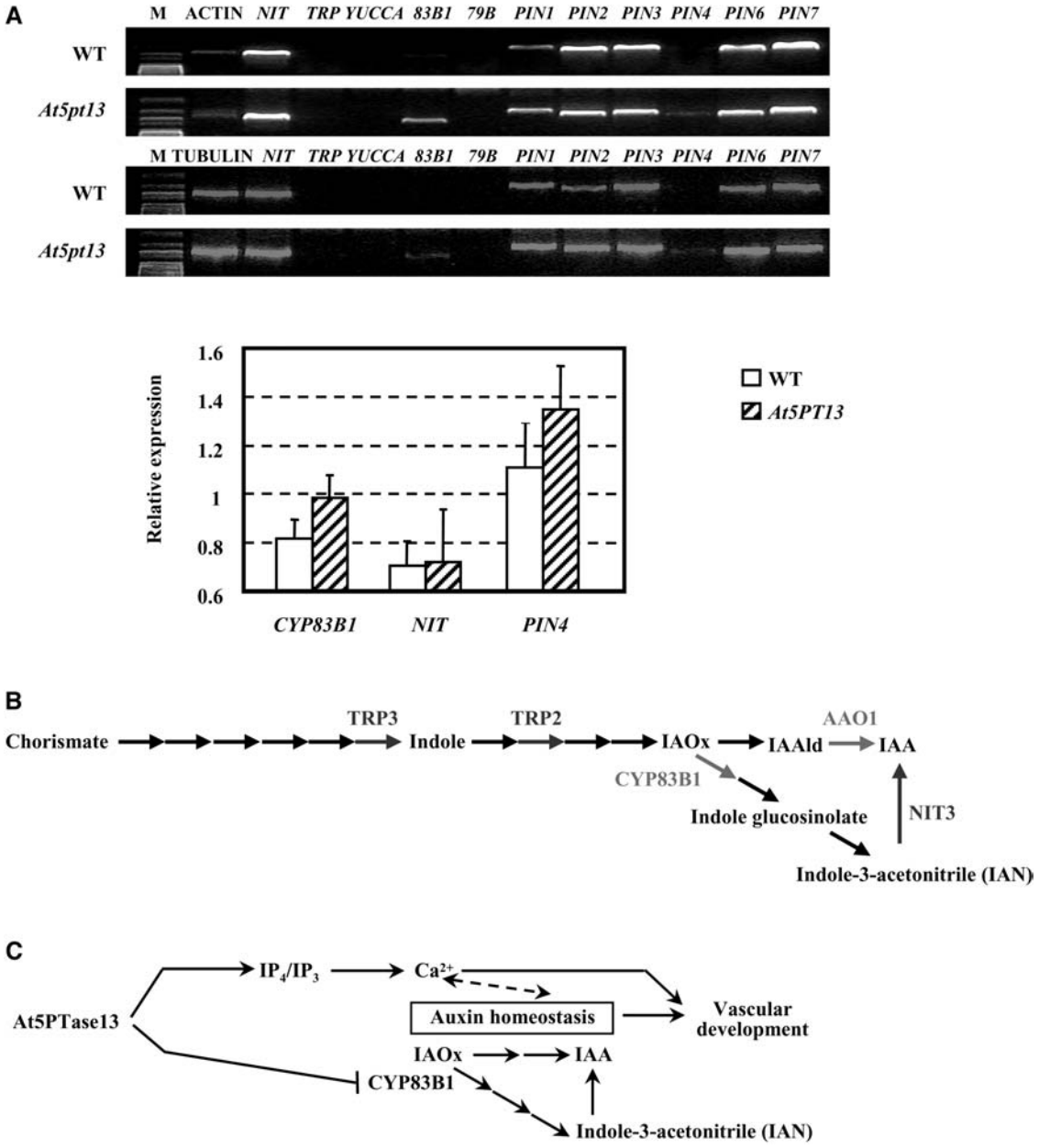

Figure 4. The *At5pt13* knockout mutation alters the expression of auxin biosynthesis- and transport-related genes. A, Semiquantitative RT-PCR analysis indicates increased expression of *CYP83B1* and *PIN4* in *At5pt13-1*. RNA was extracted from 4-d-old seedlings and PCR amplifications were performed using Arabidopsis actin or tubulin (locus nos. At3g18780 and At5g62690), respectively, as internal positive controls (bottom section). Further analysis via quantitative real-time RT-PCR confirmed the unaltered expression of *NIT1* and stimulated expression of *CYP83B1* and *PIN4* (bottom section). Data presented are compared with *AtACTIN2* and shown as percentage of the *AtACTIN2* expression. Bars indicate SD. B, Summary of the genes involved in auxin homeostasis with altered transcripts by microarray analysis. TRP3, TRP2, and NIT3 were suppressed, and CYP83B1 and AAO1 were enhanced, under *At5PTase13* deficiency. C, The hypothesized model of how At5PTase13 is involved in the cotyledon vein development through regulating auxin homeostasis and Ins(1,3,4,5)P_4-related Ca^{2+}. In normal conditions, At5PTase13 suppresses *CYP83B1* and keeps higher IAA/indole-3-acetonitrile (IAN) homeostasis. In *At5pt13-1*, release of *CYP83B1* leads to more IAN in vivo and lower IAA/IAN homeostasis. Ins(1,3,4,5)P_4-related Ca^{2+} may interact with auxin homeostasis to modulate the vascular development.

protein (ARF6, 9), are differentially regulated (Table III). These results support the involvement of At5PTase13 in auxin signal transduction as well.

Previous studies showed that overexpressed *At5PTase1* resulted in the insensitivity of transgenic plants to exogenous ABA (Sanchez and Chua, 2001). In contrast, *fry1* and *cvp2*, which were deficient in AtIPP1ase and At5PTase11, respectively, were hypersensitive to exogenous ABA, consistent with increased Ins(1,4,5)P_3 levels (Xiong et al., 2001; Carland

Table II. *Microarray analysis employing Affymetrix chip reveals the deficiency of At5PTase13 and the modification of auxin homeostasis-related genes in At5pt13-1*

The shoots of 4-d-old seedlings of wild type and *At5pt13-1* were used as samples. Numbers in the brackets indicate the regulation ratios (Log2).

Probe Set	Locus Number	Gene Symbol	Regulation
263202_at	At1g05630	*At5PTase13*	Decreased (−4)
246133_at	At5g20960	*AAO1*	Increased (0.9)
252534_at	At4g31500	*CYP83B1*	Increased (0.4)
253898_s_at	At5g54810	*TSB1/TRP2*	Decreased (−0.7)
251847_at	At3g54640	*TSA1/TRP3*	Decreased (−0.4)
252677_at	At3g44320	*NIT3*	Decreased (−1.4)

and Nelson, 2004). To explore whether *At5pt13-1* has similar phenotypes, relevant experiments were performed, and our results showed that, in contrast to *fry1* and *cvp2*, *At5pt13-1* was insensitive to exogenous ABA. As shown in Figure 5B, on the medium containing 1 or 3 μM ABA, *At5pt13-1* had much improved seed germination over the 6-d period (76% versus 31% with supplemented 3 μM ABA) compared to wild-type seeds. These results further confirm that At5PTase13 is functionally distinct from At5PTase11.

DISCUSSION

It is known that auxin and its polar transport is required for vascular differentiation and patterning in cotyledons and leaves, but the mechanisms controlling auxin accumulation and polar transport during these processes are not understood. In this study, we provide evidence that At5PTase13, a key enzyme in the PI signaling pathway, is required for normal vein formation in the cytoledon through the regulation of auxin homeostasis (probably auxin accumulation and polar

Table III. *The At5pt13-1 mutation alters the expression of genes involved in auxin signal transduction as revealed by microarray analysis*

The shoots of 4-d-old seedlings of wild type and *At5pt13-1* were used for the microarray analysis. I, Increased in *At5pt13-1*; D, decreased in *At5pt13-1*. Numbers in the brackets indicate the regulation ratios (Log2).

Probe Set	Locus No.	Regulation	Descriptions
259773_at	At1g29500	I (1.7)	Auxin-induced protein
254809_at	At4g12410	I (1.5)	Putative protein auxin-induced protein
245593_at	At4g14550	I (1.4)	IAA7-like protein
259596_at	At1g28130	I (1.3)	Auxin-regulated GH3 protein, putative similar to auxin-regulated GH3 protein
259787_at	At1g29460	I (1.3)	Auxin-induced protein
259790_s_at	At1g29430	I (1.2)	Auxin-induced protein
265182_at	At1g23740	I (1.2)	Putative auxin-induced protein
257506_at	At1g29440	I (1.1)	Auxin-induced protein
259331_at	At3g03840	I (1.1)	Putative auxin-induced protein
250012_x_at	At5g18060	I (1)	Auxin-induced protein-like
259783_at	At1g29510	I (0.9)	Auxin-induced protein
266322_at	At2g46690	I (0.6)	Putative auxin-regulated protein
251289_at	At3g61830	I (0.5)	Auxin response factor-like protein (ARF 9)
263664_at	At1g04250	I (0.5)	Putative auxin-induced protein, IAA17/AXR3-1
253255_at	At4g34760	I (0.4)	Putative auxin-regulated protein
245136_at	At2g45210	D (−3.6)	Putative auxin-regulated protein
266753_at	At2g46990	D (−2.4)	Auxin-induced protein (IAA20)
262099_s_at	At1g59500	D (−1.6)	Auxin-regulated protein GH3
253253_at	At4g34750	D (−1.3)	Putative protein auxin-regulated gene
246516_at	At5g15740	D (−1.2)	Putative protein auxin-independent growth promoter
251977_at	At3g53250	D (−1.1)	Putative protein auxin-induced protein 6B
263890_at	At2g37030	D (−0.9)	Putative auxin-induced protein
260745_at	At1g78370	D (−0.8)	2,4-D inducible glutathione S-transferase
257690_at	At3g12830	D (−0.7)	Unknown protein contains similarity to auxin-induced protein
250293_s_at	At5g13360	D (−0.6)	Auxin responsive-like protein Nt-gh3 deduced protein
256311_at	At1g30330	D (−0.6)	Auxin response factor 6 (ARF6)
266300_at	At2g01420	D (−0.6)	Putative auxin transport protein
267461_at	At2g33830	D (−0.6)	Putative auxin-regulated protein
264900_at	At1g23080	D (−0.5)	Putative auxin transport protein
253791_at	At4g28640	D (−0.4)	Early auxin-inducible protein 11 (IAA11)
256178_s_at	At1g51780	D (−0.4)	Auxin conjugate hydrolase (ILL5), identical to auxin conjugate hydrolase

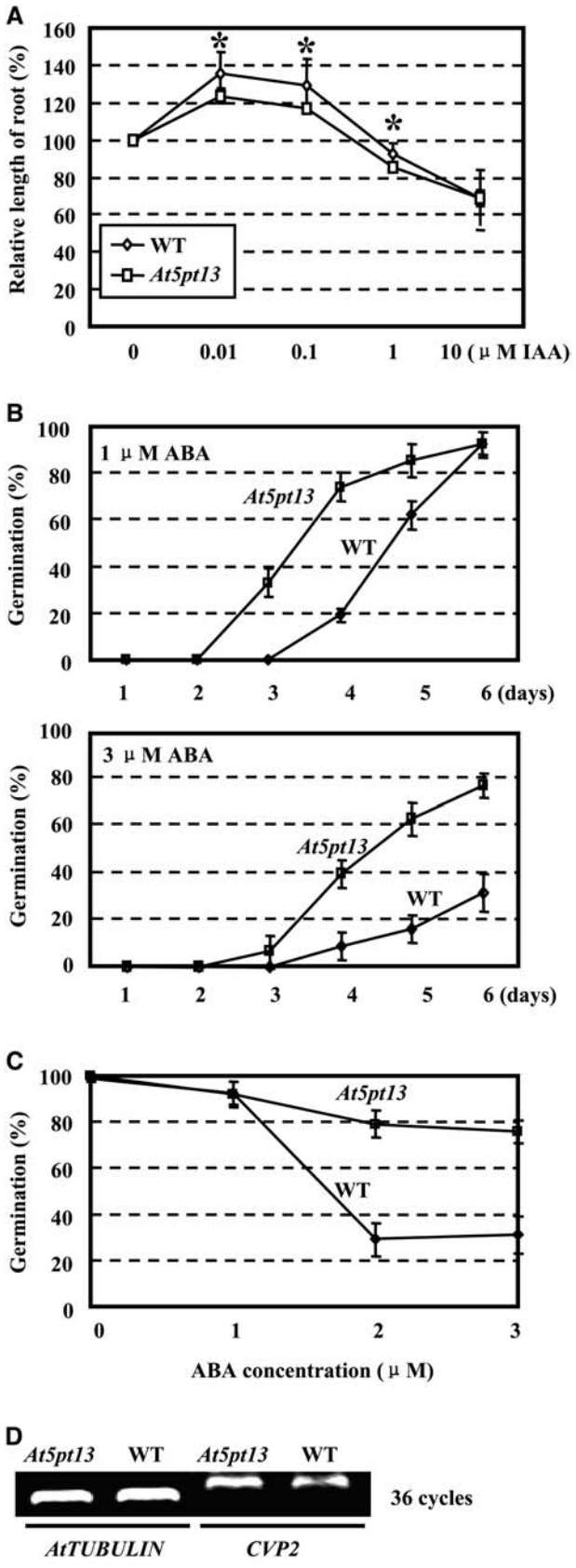

Figure 5. *At5pt13-1* is less sensitive to auxin and ABA. A, Lengths of the primary roots of 7-d-old wild-type and *At5pt13-1* seedlings on the medium supplemented with gradient auxin (0, 0.01, 0.1, 1, or 10 μM) were measured and the relative ratios of growth promoting and restraining were calculated. Error bars indicate SD, and the asterisk indicates the significant difference ($P < 0.01$) by one-tailed Student's *t* test. B, Seed germination for both wild type and *At5pt13-1* was assayed on the medium supplemented with 1 μM (top section) or 3 μM ABA (bottom section) over a 6-d period. Error bars indicate SD. C, ABA dosage effects on seed germination for both wild type and *At5pt13-1*. Squares, *At5pt13-1*; circles, wild type. Error bars indicate SD. D, Semiquantitative RT-PCR analysis indicates no changes in *CVP2* transcript levels in *At5pt13-1*. RNA was extracted from 4-d-old seedlings and PCR amplifications were performed for 36 cycles using *tubulin* (locus no. At5g62690) as internal positive control.

transport). Our data suggest that At5PTase13 appears to act in a pathway distinct from that mediated by At5PTase11, which is encoded by the *CVP2* gene that has been shown to be involved in cotyledon vein patterning in Arabidopsis (Carland et al., 1999, 2002).

At5PTase13 belongs to a plant-specific subfamily of 5PTases (Zhong and Ye, 2004). Members of this group of 5PTases contain a Trp-Asp signature (WD40 repeats), suggesting their participation in signal transduction. WD40 repeats have been shown to exist in a number of proteins, such as yeast (*Saccharomyces cerevisiae*) TUP1 (thymidine uptake 1; 5 repeats) and STE4 (a G-β-like protein; 8 repeats; Williams and Trumbly, 1990; Grotewold et al., 1991), and Arabidopsis proteins COP1 (a repressor of photomorphogenesis), SPA1 (suppressor of phyA-105), and TTG1 (*transparent testa glabra* 1; Hoecker et al., 1999; Osterlund et al., 1999; Walker et al., 1999). The WD40 domain present in COP1 interacts with transcription factors HY5 (long hypocotyl 5) and HYH (HY5 homolog), both of which are involved in light-dependent gene expression, specifically photomorphogenesis (Holm et al., 2001, 2002) and proteasome-mediated degradation (Suzuki et al., 2002). The function of the WD40 domain in At5PTase proteins is still unknown, but its presence may provide a means of protein-protein or protein-DNA interactions between At5PTase and other undefined cellular components. In addition, the presence of the WD40 domain in plant but not animal 5PTases, suggests a unique regulatory mechanism for these plant-specific 5PTases and/or their unique physiological roles in plants.

The distinction of the At5PTase13 structure from that of At5PTase11/CVP2, which lacks the WD40 domain, is consistent with the functional differences between these two 5PTases, although they both participate in vascular development. Interestingly, *At5pt13-1* and *cvp2* mutants showed opposite responses to ABA. Previous studies showed that deficiency of At5PTase1 and CVP2 resulted in the ABA hypersensitivity associated with increased Ins(1,4,5)P_3 levels. However, *At5pt13-1* showed reduced ABA sensitivity (Fig. 5, B and C). The distinct function from these two 5PTases could be explained by the differences in their substrate specificities. At5PTase11 has been shown to dephosphorylate Ins(1,4,5)P_3, thus its mutation leads to increased

accumulation of this second messenger that presumably mobilizes the release of intracellular Ca^{2+} stores. In contrast, At5PTase13 could primarily dephosphorylate Ins(1,3,4,5)P_4. It was shown that Ins(1,3,4,5)P_4 was responsible for calcium extracellular circumfluence and thus affects intracellular Ca^{2+} levels (Mishra and Delivoria-Papadopoulos, 2004).

Expression pattern analysis revealed the expression of *At5PTase13* in young seedlings, especially cotyledons, similar to the study of Zhong and Ye (2004). Genetic analysis employing a knockout mutant, *At5pt13-1*, revealed the abnormal development of cotyledon veins. An important role of *At5PTase13* and hence, inositol polyphosphate in cotyledon vein development, was further confirmed by treatment of wild-type plants with exogenous Ins(1,3,4,5)P_4 (0.01 μM; Table I), suggesting that the accumulation of the potential At5PTase13 substrate, Ins(1,3,4,5)P_4, could at least in part lead to altered cotyledon vein patterns. The occurrence of abnormal cotyledon veins that could be rescued by low concentrations of BRs or NAA (two phytohormones essential for cotyledon vein development) indicates that *At5PTase13* is involved in hormone-related cotyledon vein pattern formation. Indeed, previous studies have indicated that auxin is critical for cotyledon vein development. Deficiency of the *SHY2* gene, which encodes IAA3, a light-regulated member of the auxin-induced auxin/IAA multigene family, leads to vascular tissue deficiencies (Tian et al., 2002). Altered expression of many auxin-induced genes in this mutant indicates that SHY2/IAA3 is likely a negative factor of auxin signaling and mostly affects the primary action of auxin (Tian et al., 2002). We show that *At5pt13-1* exhibited enhanced expression of *CYP83B1* and *PIN4. CYP83B1* has been shown to decrease the level of IAA by distributing indole-3-acetaldoxime to the glucosinolate pathway, and previous studies showed that *CYP83B1*-deficient plants overaccumulated IAA, indole-3-acetaldehyde, and IAA-Asp, whereas *CYP83B1* overexpression resulted in high indole glucosinolates and low IAA (Bartel et al., 2001). These observations are consistent with the decreased auxin contents observed in *At5pt13-1* and at least in part explain how exogenous supplemented auxin rescues the abnormalities. Regarding auxin transport, PIN4-dependent auxin transport actively maintains the auxin gradient in roots, stabilizing it through a feedback loop (Friml, 2003). The increased expression of *PIN4* in *At5pt13-1* is consistent with our observation that the distribution of auxin in roots, hypocotyls, and cotyledons was altered in *At5pt13-1*. In addition to its effect on auxin distribution and accumulation, At5PTase appears to modulate auxin signaling as well, as suggested by reduced sensitivity of *At5pt13-1* to exogenous auxin and altered transcription of auxin-related genes, including those coding for auxin-induced proteins and auxin-responsive factors in this mutant.

It was suggested that CVP2 regulates cotyledon vascular development by an Ins(1,4,5)P_3 and Ca^{2+}-dependent pathway (Carland and Nelson, 2004). Furthermore, the fact that exogenous auxin could not rescue *cvp2* phenotype suggests that CVP2 mediates this process through an auxin-independent pathway. The defect in cotyledon vein patterning in *At5pt13-1* could be restored by auxin and could be mimicked by exogenous Ins(1,3,4,5)P_4, implying the involvement of At5PTase13 in both Ca^{2+}- and auxin-dependent vascular development. Further studies will be necessary to test this hypothesis.

In conclusion, we have demonstrated that AtPTase13 modulates cotyledon vein patterning via the regulation of auxin homeostasis, a mechanism that is distinct from the one that underlies AtPTase11/CVP2 modulation of cotyledon vein development. Arabidopsis contains a multigene family of 5PTases (Berdy et al., 2001; Ercetin and Gillaspy, 2004; Zhong et al., 2004). Our analysis showed that in addition to *At5PTase13*, five other *At5PTase* genes are transcribed in cotyledons (W.-H. Lin and H.-W. Xue, unpublished data). An interesting question is whether these At5PTases are also involved in the regulation of vascular development. In the future, detailed studies on the expression patterns of the various *5PTase* genes, their knockout phenotypes, and their substrate specificities will provide insights into this question.

MATERIALS AND METHODS

Enzymes and Compounds

Enzymes used for DNA manipulation were purchased from Boehringer Mannheim and New England Biolabs. DNA primers used for PCR were obtained from TibMolbiol. D-*myo*-inositol 1,3,4,5-tetraphosphate (sodium) was obtained from Echelon.

Bacteria and Plants

Escherichia coli strain XL-1 Blue (Stratagene) was used for DNA cloning and library screening. Arabidopsis (*Arabidopsis thaliana*) L. Heglu (Columbia ecotype) seeds were surface sterilized with 20% bleach and washed four times with sterile water, then germinated on agar medium containing half-strength Murashige and Skoog salts. Plants were then placed in soil and grown in a phytotron with a 16-h-light (22°C) and 8-h-dark (18°C) cycle. For phytohormone treatments, 7-d-old seedlings were treated with 100 μM auxin (IAA), 100 μM cytokinin (Kinetin), 100 μM GA (GA3), or 1 μM 24-eBL for 8 h. Exogenous 0.1 μM NAA (Sigma) or 0.1 μM 24-eBL (Sigma) were used for supplementing phytohormones during seedling growth. Plant crosses were carried out by removal of the petals, sepals, and androecia from large green buds and subsequent artificial fecundation at 12 PM to 3 PM over the next 2 d. Arabidopsis plants were transformed by floral dipping into *Agrobacterium tumefaciens* GV3101 strains containing binary vectors. For the seed germination assay, 50 seeds from wild-type and *At5pt13-1* plants were sowed on Murashige and Skoog medium containing different concentrations of ABA (0, 1, 2, and 3 μM). Seeds were regarded as germinated when radicle completely penetrated the seed coat, and germination was scored daily up to 6 d after being placed at room temperature. For the seeding hormone sensitivity assay, lengths of primary roots of 7-d-old wild-type and *At5pt13* seedlings on the medium supplemented with gradient auxin (0, 0.01, 0.1, 1, or 10 μM) were measured, and the relative ratios of growth promoting and restraining were calculated. The experiments were repeated in duplicates.

Isolation of At5PTase13 cDNA

DNA manipulation was performed using standard protocols (Sambrook et al., 1989). The cDNA sequence coding for an inositol polyphosphate 5Ptase (AJ005682; H.-W. Xue, unpublished data) was used as probe to search against

the National Center for Biotechnology Information database (http://www.ncbi.nlm.nih.gov/dbEST/index.html), resulting in the identification of a putative inositol polyphosphate 5Ptase coding region from Arabidopsis (accession no. AC007153). Specific primers located in the predicted first exon (At5PT-1, 5′-CGAAGAAGAAGACGAAGAGGCG-3′ and At5PT-2, 5′-GGAGACACGCTCCTTGAAAGG-3′) were designed and used for PCR amplification. The resulting PCR product was used to isolate the corresponding cDNAs from an Arabidopsis hypocotyl cDNA library via a PCR-based strategy (Alfandari and Darribere, 1994), and plaque-purified phage clones were converted to pBluescript derivatives using ExAssist helper phage according to the supplier's instructions (Stratagene). The clone containing the longest cDNA insert (pAt5PTase13) was used for further analysis. DNA sequencing was performed by Genecore and computational analysis was based on the programs of the Wisconsin Genetics Computer Group (GCG package, version 10.1).

Semiquantitative RT-PCR Analysis and Promoter-Reporter Gene Fusion Studies

Semiquantitative RT-PCR was used to study the mRNA expression of *At5PTase13* in various tissues. Total RNAs from 4-d-old seedlings, cotyledons, 3-week-old rosette leaves, roots, flowers, and stems after 1 week flowering were extracted with the Trizol reagent (Gibco-BRL) and reverse transcribed with oligo(dT) primers (TaKaRa RT-kit). The resulting cDNA products were used as templates for PCR amplification, with Arabidopsis actin-coding cDNA (gene locus no. At1g49240) used as an internal positive control with primers aAct-1 (5′-GCGGTTTTCCCCAGTGTTGTTG-3′) and 2 (5′-TGCCTGGACCTGCTTCATCATACT-3′). PCR reactions were as follows: 94°C for 2 min; followed by 32 or 36 cycles of 94°C for 1 min, 56°C for 45 s, and 72°C for 1 min, with a final extension at 72°C for 10 min. The resulting PCR products were resolved on 1% to 2% agarose gels and assessed using a Gel Doc 2000 system (Bio-Rad).

The expression pattern of *At5PTase13* was further analyzed using transgenic expression of the promoter-reporter gene fusion. A 1.4-kb genomic DNA region in front of the translation initiation site ATG was analyzed for the presence of cis-regulatory elements, and then PCR amplified with primers At5PT13pro-1 (5′-TTGATGTGTACTATGATTATCATC-3′) and At5PT13pro-2 (5′-CGACAATCAGAGGAATTCAAG-3′). The amplified DNA fragment was confirmed by sequencing and then subcloned into pBI101 vector (General Biomass) to yield the construct harboring this region fused to a reporter gene (*E. coli GUS*). This construct (pBI101-P) was transformed into Arabidopsis. T_0 transgenic seedlings were screened on Murashige and Skoog medium supplemented with 30 mg/L kanamycin, and T-DNA integration was confirmed by PCR analysis using primers annealing to the kanamycin resistance gene (NPTII-s, 5′-AGAGGCTATTCGGCTATGACTGG-3′ and NPTII-a, 5′-ATCGCCATGGGTCACGACGAGAT-3′). 1-, 2-, 3-, 5-, and 7-d-old seedlings of T2 homozygous plants were analyzed for GUS activities as described by Jefferson et al. (1987), with an SMZ 800 stereoscope (Nikon).

Identification of an *At5PTase13* Knockout Mutant

The *At5PTase13* genomic sequence was used to BLAST search the flanking sequences database of the Arabidopsis mutation populations offered by Syngenta (http://www.syngenta.com), resulting in the identification of an insertion line, Garlic 350-F1. Mutant seeds were screened in one-half Murashige and Skoog medium containing 20 mg/L Basta for calculating the segregation ratio and homozygous lines and were confirmed through PCR amplification with primers At5PT13conf-1 (5′-CGGGGATCCAAGGAAACTTTATATGCCAG-3′) and At5PT13conf-2 (5′-CACATGGAACTGCTGCAACATC-3′) in combination with the T-DNA-specific primer (LB3).

To confirm the *At5PTase13* deficiency, total RNA was extracted from 4-d-old mutant and wild-type seedlings, reverse transcribed, and used as templates for RT-PCR analyses using primers At5PT13defi-1 (5′-AAGCGAATTCCTGCGTGGTGTG-3′) and At5PT13defi-2 (5′-TTCTTTGTTAGGTTCGTGGGTCTG-3′). The experiments were repeated three times with independent samples. The knockout mutant was designated as *At5pt13-1*.

Phenotypic Analysis of *At5pt13-1*

Cotyledon veins of 2-, 4-, and 6-d-old *At5pt13-1* mutant and wild-type seedlings were observed. The cotyledons were cleared in 95% ethanol to remove chlorophyll and fixed with formaldehyde-acetic acid buffer (50% ethanol, 5% acetic acid, 3.7% formaldehyde, and 41.3% water) for at least 15 min. Before observation with an SMZ 800 stereoscope, the materials were treated overnight with HCG clearing solution (Sabatini et al., 1999). Structures of the cotyledon veins were observed using differential interference contrast optics (Leica DMR microscope equipped with a Leica DC 300F digital camera). The numbers of cotyledons with abnormal veins were counted and ratios (the percentage of cotyledons with abnormal veins of the total observed cotyledons) were calculated.

Complementation of the *At5pt13-1* Mutant

The full-length *At5PTase13* cDNA was subcloned into construct pBI101-P precut with *Xba*I and *Sal*I, and the resulting construct containing *At5PTase13* cDNA under its own native promoter (pBI101-P-At5PTase13) was transformed into wild-type and homozygous mutant plants. The T_0 seeds were screened on medium containing 30 mg/L kanamycin and the resistant plants were confirmed to be transgenics by PCR amplification using primers annealing to the kanamycin resistance gene (NPTII-s and NPTII-a). The rescued expression of *At5PTase13* in mutant plants was confirmed through semiquantitative RT-PCR using primers At5PT13defi-1 and -2. The cotyledons were dissolved by 95% ethanol and fixed by formaldehyde-acetic acid, and then observed.

Measurement of Auxin Content in Seedlings

To measure auxin contents, 4-d-old wild-type and *At5pt13* seedlings were sampled with a mortar and pestle, and similar amounts of samples (300 mg of fresh weight) were used for the measurement of IAA contents. IAA was extracted by 80% methanol and centrifugated at 5,000*g* for 10 min at 4°C. The supernatant was collected and immediately applied to a pre-equilibrated C_{18} Sep-Pak cartridge (Millipore), which was washed with 70% methanol solution. After methyl-esterification with diazomethane, the free IAA content was measured by ELISA (as described by Liang and Yin, 1994). In detail, 96-well immunoassay plates were coated with mouse anti-IAA monoclonal antibody (0.1 mL, 1:10,000) in 50 mM NaHCO3 (pH 9.6) at 37°C overnight with 100% humidity. Standard curve was generated under different concentrations of IAA standard buffer (1,000, 250, 62.5, 15.63, 3.9, and 0.98 pmol/50 μL). After incubation, the supernatant was discarded and the plates were washed twice (phosphatic buffer) and then incubated with Ovalbumin at 37°C for 30 min. After further wash and dispensation of IAA standard buffers, the plates were incubated with horseradish peroxidase-linked rabbit anti-mouse (1:20,000) in 50 mM $NaHCO_3$ (pH 9.6) at 37°C for 70 min. The conjugate was removed by washing and optical densities were measured at 490 nm.

Semiquantitative RT-PCR Analysis of mRNA Expression of Auxin Biosynthesis- and Transport-Related Genes

Expression of genes encoding auxin biosynthesis- and transport-related proteins in *At5pt13* plants was analyzed using semiquantitative RT-PCR. The selected genes and the relevant primer sequences were as follows: *FMO/YUCCA* (flavin-containing monooxygenase, At4g32540, YUCCA-s, 5′-ACACGGTCCCATCATCATCG-3′, and YUCCA-a, 5′-AAGCCAAGTAGGCACGTTGC-3′); *CYP79B* (cytochrome P450 family member, At1g05090, CYP79B-s, 5′-CCGGTTTCGGTACGATTGTC-3′, and CYP79B-a, 5′-TGCTTGACCCATCCGTTTC-3′); *CYP83B1* (cytochrome P450 monooxygenase, At4g31500, CYP83B1-s, 5′-AAGGGCAACAAACCATGTCG-3′, and CYP83B1-a, 5′-TTGGCCGGAATATCATAGCC-3′); *NIT1* (At3g44310, NIT1-s, 5′-TTCGGTTTAGCGGTTGGC-3′, and NIT1-a, 5′-TCGGGTGCTCATTTACGGTC-3′); *Trp-2* (TSB1, Trp synthase, β-subunit 1, At5g54810, Trp-2-s, 5′-TCCGTTTCTTCAGCTCCTTCC-3′, and Trp-2-a, 5′-TTTGCCACTGTCCAATCCG-3′); *PIN1* (At1g73590, PIN1-s, 5′-ATGAGCGAGGATCTCTATGG-3′, and PIN1-a, 5′-AACAGGCGCATTGTCACCCG-3′); *PIN2* (At5g57090, PIN2-s, 5′-ATCAGGAAGGATCTCTATGG-3′, and PIN2-a, 5′-AATAGCTGCATTGTCACCCG-3′); *PIN3* (At1g70940, PIN3-s, 5′-TTACTGCGTGTCGCTATAGT-3′, and PIN3-a, 5′-GAGTTACCCGAACCTAATCA-3′); *PIN4* (At2g01420, PIN4-s, 5′-TCATTGCTTGTGGGAACTCT-3′, and PIN4-a, 5′-ACCACTTAACTAGAAACTTCA-3′); *PIN6* (At1g77110, PIN6-s, 5′-TCATTGCTTGATGCCACCATGAAGT-3′, and PIN6-a, 5′-ACCACTTAACTACGGTGGTACTTCA-3′); and *PIN7* (At1g23080, PIN7-s, 5′-CGGTAAACATAATGCCACCA-3′, and PIN7-a, 5′-TCTAGTTGCGTTCCACTAATC-3′). PCR amplifications were performed using Arabidopsis actin2 or tubulin2 (locus nos. At3g18780 and At5g62690) as internal positive controls, respectively.

Real-Time Quantitative RT-PCR Analysis

Quantitative RT-PCR analyses were performed to study the transcription levels of *At5PTase13* in various tissues (with primers RTs, 5′-GTAAAAGTGGATTTGATACATAAGAT-3′, and RTa, 5′-ATGGGCTAGATTGAGTGTCTCT-3′) and the auxin biosynthesis-related genes (with primers AtCYP83B1RTs, 5′-TTGGATATTGTTGTGCCGGG-3′, and a, 5′-GAGCCGAAGAGACTCCTTGATG-3′; AtNIT1RTs, 5′-AAGATTGGCTGACGTGGCTAGG-3′, and a, 5′-AATGGGAGTGTCGTAAACGGG-3′) and auxin polar transport genes (AtPIN4RTs, 5′-AACCGGTACGGGTGTTTCAAC-3′, and a, 5′-TGATCAGAGACAACCATCCG-3′) in Arabidopsis seedlings of wild type and *At5pt13*. Total RNA was isolated from Arabidopsis 4-d-old seedlings using the Trizol reagent (Huashun) and reverse transcribed in a total volume of 20 μL using 2 μg total RNA as template and incubated at 42°C for 45 min (SuperScript preamplification system, Promega). RT-PCR was performed and Arabidopsis actin2 encoding gene (locus no. At3g18780) was used as internal control with primers AtACTIN2s (5′-CCTTCGTCTTGATCTTGCGG-3′) and a (5′-AGCGATGGCTGGAACAGAAC-3′).

Real-time quantitative RT-PCR was then carried out by RotorGene 3000 (Corbett Research) using a SYBR green detection protocol (SYBR Premix Ex Taq system, TaKaRa). The product amounts were determined each cycle by the RotorGene software. Differences of cycles during the linear amplification phases between diverse samples, which compared with the transcript of *AtACTIN2*, respectively, were used to examine relative expression levels of the tested genes.

Expression Profiling of Genes in *At5pt13-1* Seedlings Using Microarray Analysis

Shoots of 4-d-old *At5pt13-1* and wild-type plants were harvested and RNA samples were prepared according to the protocols by manufacturers (Affymetrix). Briefly, total RNA was extracted and 2 μg of poly(A)$^+$-mRNA was converted to double-stranded cDNA using the SuperScript polymerase II (Affymetrix) with a T7-(dT)24 primer incorporating a T7 RNA polymerase promoter (Genset). Biotin-labeled cRNA was synthesized in vitro and 15 μg of which was purified and fragmented into 35- to 300-bases pieces and then hybridized with an Arabidopsis genome array (Affymetrix ATH1). After removal of the hybridization mixture, the arrays were washed, stained with streptavidin-phycoerythrin (Molecular Probes, Affymetrix), and biotinylated with goat anti-streptavidin antibody (Vector Laboratories) in the Affymetrix fluidics stations using standard procedures. Arrays were scanned using an Agilent GeneArray scanner (Affymetrix), and the resulting data were normalized using the Affymetrix Microarray Suite program (version 5.0) and set the algorithm absolute call flag, indicating the reliability of the data points according to P (present) and A (absent). The significant difference ($P < 0.003$) of each gene between the wild type and *At5pt13* was examined using the Wilcoxon rank test of the Affymetrix Microarray Suite program. The genes with the consensus significant difference were selected and analyzed by a strict screening criteria, of which at least 1-fold variation (log ratio >0.4 for up-regulated genes, and <-0.4 for down-regulated ones) was detected. Finally, the annotations for the selected probe-sets ID were rechecked at the Affymetrix Web site (http://www.Affymetrix.com). The hybridizations were repeated with independent samples.

Accession Numbers

Nucleotide sequences reported in this paper have been submitted to the GenBank/EMBL Data Bank under accession numbers AJ297426 (*At5PTase13*), NM_112764 (*Actin2*), and M20405 (*β-tubulin2*).

ACKNOWLEDGMENT

We greatly thank Mr. Jian Xu (Utrecht University, The Netherlands) for providing the Arabidopsis seeds containing the DR5-GUS construct.

Received June 14, 2005; revised July 22, 2005; accepted August 24, 2005; published November 18, 2005.

LITERATURE CITED

Alfandari D, Darribere T (1994) A simple PCR method for screening cDNA libraries. PCR Methods Appl **4:** 46–49

Bak S, Tax FE, Feldmann KA, Galbraith DW, Feyereisen R (2001) CYP83B1, a cytochrome P450 at the metabolic branch point in auxin and indole glucosinolate biosynthesis in Arabidopsis. Plant Cell **13:** 101–111

Bartel B, LeClere S, Magidin M, Zolman BK (2001) Inputs to the active indole-3-acetic acid pool: de novo synthesis, conjugate hydrolysis, and indole-3-butyric acid β-oxidation. J Plant Growth Regul **20:** 198–216

Berdy SE, Kudla J, Gruissem W, Gillaspy GE (2001) Molecular characterization of At5PTase1, an inositol phosphatase capable of terminating inositol trisphosphate signaling. Plant Physiol **126:** 801–810

Burnette RN, Gunesekera BM, Gillaspy GE (2003) An Arabidopsis inositol 5-phosphatase gain-of-function alters abscisic acid signaling. Plant Physiol **132:** 1011–1019

Carland FM, Berg BL, FitzGerald JN, Jinamornphongs S, Nelson T, Keith B (1999) Genetic regulation of vascular tissue patterning in Arabidopsis. Plant Cell **11:** 2123–2137

Carland FM, Fujioka S, Takatsuto S, Yoshida S, Nelson T (2002) The identification of CVP1 reveals a role for sterols in vascular patterning. Plant Cell **14:** 2045–2058

Carland FM, Nelson T (2004) COTYLEDON VASCULAR PATTERN2-mediated inositol (1,4,5) trisphosphate signal transduction is essential for closed venation patterns of Arabidopsis foliar organs. Plant Cell **16:** 1263–1275

Deyholos MK, Cordner G, Beebe D, Sieburth LE (2000) The SCARFACE gene is required for cotyledon and leaf vein patterning. Development **127:** 3205–3213

Ercetin ME, Gillaspy GE (2004) Molecular characterization of an Arabidopsis gene encoding a phospholipid-specific inositol polyphosphate 5-phosphatase. Plant Physiol **135:** 938–946

Erneux C, Govaerts C, Communi D, Pesesse X (1998) The diversity and possible functions of the inositol polyphosphate 5-phosphatases. Biochim Biophys Acta **1436:** 185–199

Friml J (2003) Auxin transport—shaping the plant. Curr Opin Plant Biol **6:** 7–12

Grotewold E, Athma P, Peterson T (1991) Alternatively spliced products of the maize P gene encode proteins with homology to the DNA-binding domain of myb-like transcription factors. Proc Natl Acad Sci USA **88:** 4587–4591

Hatzack F, Hubel F, Zhang W, Hansen PE, Rasmussen SK (2001) Inositol phosphates from barley low-phytate grain mutants analysed by metal-dye detection HPLC and NMR. Biochem J **354:** 473–480

Hobbie L, McGovern M, Hurwitz LR, Pierro A, Liu NY, Bandyopadhyay A, Estelle M (2000) The axr6 mutants of *Arabidopsis thaliana* define a gene involved in auxin response and early development. Development **127:** 23–32

Hoecker U, Tepperman JM, Quail PH (1999) SPA1, a WD-repeat protein specific to phytochrome A signal transduction. Science **284:** 496–499

Holm M, Hardtke CS, Gaudet R, Deng XW (2001) Identification of a structural motif that confers specific interaction with the WD40 repeat domain of *Arabidopsis* COP1. EMBO J **20:** 118–127

Holm M, Ma LG, Qu LJ, Deng XW (2002) Two interacting bZIP proteins are direct targets of COP1-mediated control of light-dependent gene expression in *Arabidopsis.* Genes Dev **16:** 1247–1259

Jefferson RA, Kavanagh TA, Bevan MW (1987) GUS fusions: beta-glucuronidase as a sensitive and versatile gene fusion marker in higher plants. EMBO J **6:** 3901–3907

Koizumi K, Sugiyama M, Fukuda H (2000) A series of novel mutants of *Arabidopsis thaliana* that are defective in the formation of continuous vascular network: calling the auxin signal flow canalization hypothesis into question. Development **127:** 3197–3204

Liang HY, Yin WL (1994) Assay of exogenous IAA, ABA and GA_{1+3} of shoots of leaf and flower in *Metasequoia glyptostroboides* Hu et Cheng. Forest Science and Technology **11:** 13–15

Lin WH, Ye R, Ma H, Xu ZH, Xue HW (2004) DNA chip-based expression profile analysis indicates involvement of the phosphatidylinositol signaling pathway in multiple plant responses to hormone and abiotic treatments. Cell Res **14:** 34–45

Mattsson J, Sung ZR, Berleth T (1999) Responses of plant vascular systems to auxin transport inhibition. Development **126:** 2979–2991

Mishra OP, Delivoria-Papadopoulos M (2004) Inositol tetrakisphosphate (IP_4)- and inositol triphosphate (IP_3)-dependent Ca^{2+} influx in cortical neuronal nuclei of newborn piglets following graded hypoxia. Neurochem Res **9:** 391–396

Osterlund MT, Ang LH, Deng XW (1999) The role of COP1 in repression of *Arabidopsis* photomorphogenic development. Trends Cell Biol **9:** 113–118

Pouillon V, Hascakova-Bartova R, Pajak B, Adam E, Bex F, Dewaste V, VanLint C, Leo O, Erneux C, Schurmans S (2003) Inositol 1,3,4, 5-tetrakisphosphate is essential for T lymphocyte development. Nat Immunol **4:** 1136–1143

Sabatini S, Beis D, Wolkenfelt H, Murfett J, Guilfoyle T, Malamy J, Benfey P, Leyser O, Bechtold N, Weisbeek P, et al (1999) An auxin-dependent distal organizer of pattern and polarity in the *Arabidopsis* root. Cell **99:** 463–472

Sambrook PN, Champion GD, Browne CD, Cairns D, Cohen ML, Day RO, Graham S, Handel M, Jaworski R, Kempler S (1989) Corticosteroid injection for osteoarthritis of the knee: peripatellar compared to intra-articular route. Clin Exp Rheumatol **7:** 609–613

Sanchez JP, Chua NH (2001) Arabidopsis PLC1 is required for secondary responses to abscisic acid signals. Plant Cell **13:** 1143–1154

Semiarti E, Ueno Y, Tsukaya H, Iwakawa H, Machida C, Machida Y (2001) The ASYMMETRIC LEAVES2 gene of Arabidopsis thaliana regulates formation of a symmetric lamina, establishment of venation and repression of meristem-related homeobox genes in leaves. Development **128:** 1771–1783

Sieburth LE (1999) Auxin is required for leaf vein pattern in Arabidopsis. Plant Physiol **121:** 1179–1190

Suzuki G, Yanagawa Y, Kwok SF, Matsui M, Deng X-W (2002) *Arabidopsis* COP10 is a ubiquitin-conjugating enzyme variant that acts together with COP1 and the COP9 signalosome in repressing photomorphogenesis. Genes Dev **16:** 554–559

Tian Q, Uhlir NJ, Reed JW (2002) Arabidopsis SHY2/IAA3 inhibits auxin-regulated gene expression. Plant Cell **14:** 301–319

Ulmasov T, Murfett J, Hagen G, Guilfoyle TJ (1997) Aux/lAA proteins repress expression of reporter genes containing natural and highly active synthetic auxin response elements. Plant Cell **9:** 1963–1971

Walker AR, Davison PA, Bolognesi-Winfield AC, James CM, Srinivasan N, Blundell TL, Esch JJ, Marks MD, Gray JC (1999) The *TRANSPARENT TESTA GLABRA1* locus, which regulates trichome differentiation and anthocyanin biosynthesis in Arabidopsis, encodes a WD40 repeat protein. Plant Cell **11:** 1337–1350

Williams FE, Trumbly RJ (1990) Characterization of TUP1, a mediator of glucose repression in *Saccharomyces cerevisiae.* Mol Cell Biol **10:** 6500–6511

Xiong L, Lee B, Ishitani M, Lee H, Zhang C, Zhu JK (2001) FIERY1 encoding an inositol polyphosphate 1-phosphatase is a negative regulator of abscisic acid and stress signaling in *Arabidopsis.* Genes Dev **15:** 1971–1984

Ye ZH, Varner JE (1991) Tissue-specific expression of cell wall proteins in developing soybean tissues. Plant Cell **3:** 23–37

Zhong R, Burk DH, Morrison WH, Ye ZH (2004) FRAGILE FIBER3, an Arabidopsis gene encoding a type II inositol polyphosphate 5-phosphatase, is required for secondary wall synthesis and actin organization in fiber cells. Plant Cell **16:** 3242–3259

Zhong R, Ye Z-H (2004) Molecular and biochemical characterization of three WD-repeat-domain-containing inositol polyphosphate 5-phosphatases in *Arabidopsis thaliana.* Plant Cell Physiol **45:** 1720–1728

Zhu DM, Tekle E, Huang CY, Chock PB (2000) Inositol tetrakisphosphate as a frequency regulator in calcium oscillations in HeLa cells. J Biol Chem **275:** 6063–6066